2009 American Control Conference
Hyatt Regency Riverfront, St. Louis, MO, USA
June 10-12, 2009



# Path Following Using Transverse Feedback Linearization: Application to a Maglev Positioning System

Christopher Nielsen, Cameron Fulford and Manfredi Maggiore

*Abstract*— **This article presents an approach to path following control design based on transverse feedback linearization. A "transversal" controller is designed to drive the output of the plant to the path. A "tangential" controller meets application-specific requirements on the path, such as speed regulation and internal stability. This methodology is applied to a five degree-of-freedom (5-DOF) magnetically levitated positioning system. Experimental results demonstrate the effectiveness of our control design.**

## I. Introduction

The path following control problem (PFP) is chiefly concerned with providing a stable motion along a given path with no *a priori* time parameterization associated with the movement on the path. More specifically, the control objective is to drive the output of a control system to the path in such a way that the path is traversed in a desired direction. Usually, specific applications impose additional requirements, such as speed regulation on the path and internal stability.

PFP has some affinity to the tracking control problem, in which it is desired that the system output asymptotically matches a reference signal, but there are fundamental differences. Tracking controllers stabilize a specific system trajectory, while path following controllers should stabilize a *family* of trajectories, all those whose associated output signals lie on the desired path. We call the collection of all such trajectories the *path following manifold*. Its precise definition is given in Section II.

The point of view taken in this paper is to convert PFP into the stabilization of the path following manifold. This guarantees, among other things, an invariance property : if the state is appropriately initialized, then the resulting output signal lies on the desired path at all time. Among various possible set stabilization techniques, we choose to use transverse feedback linearization [1], [8], [9], which makes it possible to divide the control design into two steps: the stabilization of the path following manifold (transversal control design) and the control of the motion on the manifold (tangential control design).

We apply this methodology to the design of a path following controller for a 5-DOF magnetically levitated system at the University of Toronto Systems Control research lab. The control objective is to make a platen move along a closed Jordan curve defined within the system's range of operation.

The path invariance property induced by our control method is particularly beneficial in this application, because it effectively creates virtual mechanical constraints in the system that make it act as if it were being guided by (reconfigurable) mechanical guides. This distinguishes our path following controller from some others in the literature. Due to a lack of space, we regrettably omit a literature review on solutions to the path following problem.

The following notation is used in this paper. We denote by $I_m$ the $m \times m$ identity matrix and by $0_{m\times n}$ the $m \times n$ matrix of zeros. Let $\mathrm{col}(x_1, \ldots, x_k) := [x_1 \ \ldots \ x_k]^\top$.

## II. Path following methodology

We consider smooth control-affine systems with $m$ inputs and $p$ outputs,

$$\begin{aligned} \dot{x} &= f(x) + g(x)u \\ y &= h(x). \end{aligned} \tag{1}$$

Given a smooth embedded[1]path in the output space, $\gamma := \{y : s(y) = 0\}$, we want to design a smooth feedback that makes the output of the system (1) approach and traverse $\gamma$ in a desired direction with a desired speed. Moreover, it is required that $\gamma$ be output invariant for the closed-loop system. In order to give a precise definition of output invariance, let $\Gamma := \{x : s(h(x)) = 0\}$. Stabilizing the set $\Gamma$ corresponds to sending the output of the plant to the desired path. However, generally $\Gamma$ is not an invariant set so one should instead stabilize the maximal controlled-invariant set contained in $\Gamma$, denoted by $\Gamma^\star$. Intuitively, the set $\Gamma^\star$ is the collection of all those motions of the control system (1) whose associated output signals can be made to lie in $\gamma$ at all time by a suitable choice of input signal. Assume that $\Gamma^\star$ is non-empty (this is a basic feasibility requirement for the path following problem) and it is a closed embedded submanifold of the state space. Let $n^\star := \dim(\Gamma^\star)$. With this assumption, $\Gamma^\star$ is precisely the zero dynamics manifold of the control system $\dot{x} = f(x) + g(x)u$ with output $\hat{y} = s(h(x))$. We call $\Gamma^\star$ the *path following manifold*. Given a smooth feedback $u(x)$, we say that $\gamma$ is *output invariant* for the closed-loop system if $\Gamma^\star$ is an invariant set with respect to the vector field $f(x) + g(x)u(x)$.

C. Fulford was partially supported by the National Science and Engineering Research Council of Canada (NSERC) and the Canadian Fund for Innovation (CFI). C. Nielsen and M. Maggiore were supported by NSERC. The authors wish to thank Jacob Apkarian at Quanser for his help and support.

The authors are with the Department of Electrical and Computer Engineering, University of Toronto, 10 King's College Road, Toronto, ON, M5S 3G4, Canada. {nielsen, fulford, maggiore}@control.toronto.edu

[1]By *smooth* we mean that $s$ is a smooth function; by *embedded* we mean that the path has no self-intersections and it is a closed subset of $\mathbb{R}^p$. This is equivalent to requiring that one can choose $s : \mathbb{R}^p \to \mathbb{R}^{p-1}$ so that its Jacobian has full rank $p-1$ everywhere on $\gamma$.

The path following control design problem entails finding a feedback ensuring that three objectives are met.

- **P1** For each initial condition in a suitable set, the corresponding solution $x(t)$ is defined for all $t \geq 0$ and $\|h(x(t))\|_\gamma \to 0$ as $t \to +\infty$, where $\|y\|_\gamma$ denotes the point-to-set distance of $y$ to the set $\gamma$, i.e., $\|y\|_\gamma := \inf_{p\in\gamma} \|y - p\|$.
- **P2** The set $\gamma$ is output invariant for the closed-loop system.
- **P3** The motion on $\gamma$ meets additional application-specific requirements such as direction and speed of traversal of the path, and boundedness of the internal dynamics.

Our approach to solving PFP is summarized below.

- **S1** Find the path following manifold $\Gamma^\star$.
- **S2** Transverse feedback linearization, [9] [7]. Find, if possible, a coordinate transformation $T : x \mapsto (\eta, \xi)$, defined in a neighbourhood $U$ of $\Gamma^\star$, and a regular feedback transformation $u = \alpha(x) + \beta(x)v$ ($\beta$ non-singular on $U$) such that $T(\Gamma^\star) = \{(\eta, \xi) : \xi = 0\}$ and, in new coordinates,

$$\begin{aligned} \dot\eta &= f^0(\eta, \xi) + g^\pitchfork(\eta, \xi)v^\pitchfork + g^\parallel(\eta, \xi)v^\parallel \\ \dot\xi &= A\xi + Bv^\pitchfork \end{aligned} \tag{2}$$

  with $v = \mathrm{col}(v^\pitchfork, v^\parallel) \in \mathbb{R}^m$ and $(A, B)$ a controllable pair. We refer to the $\xi$ subsystem as the *transversal subsystem*. On the other hand, the system $\dot\eta = f^0(\eta, 0) + g^\parallel(\eta, 0)v^\parallel$ is the *tangential subsystem*.
- **S3** Transversal control design. Design a transversal feedback $v^\pitchfork(\xi)$ stabilizing the origin of the transversal subsystem.
- **S4** Tangential control design. Design a tangential feedback $v^\parallel(\eta, \xi)$ such that, when $\xi = 0$, the tangential subsystem meets the application-specific goals in **P3** and, moreover, the closed-loop system has no finite escape times.

The approach outlined above relies on the stabilization of the path following manifold $\Gamma^\star$. Other set stabilization approaches may be used to stabilize $\Gamma^\star$, but transverse feedback linearization is particularly well suited to path following in that it allows one to separately address the stabilization of $\Gamma^\star$ (objectives **P1** and **P2**) and the control of the dynamics on $\Gamma^\star$ (objective **P3**). More specifically, the tangential subsystem, with state $\eta$, describes the motion on $\Gamma^\star$, that is when the plant output lies in $\gamma$. The tangential controller is designed to meet goal **P3**. The transversal subsystem, with state $\xi$, describes the motion off the set $\Gamma^\star$. Due to the absence of finite escape times, the transversal controller stabilizes $T(\Gamma^\star)$. If the trajectories of the closed-loop system are bounded[2], then the stabilization of $T(\Gamma^\star)$ implies that of $\Gamma^\star$, and therefore the transversal controller meets goal **P1**. It also meets goal **P2** because the origin of the $\xi$ subsystem is an equilibrium of the closed-loop system, and thus $\Gamma^\star$ is an invariant set of the closed-loop system.

[2]It may happen in some applications that the trajectories of the closed-loop system aren't bounded because the path itself is unbounded. In this case, in order to be able to state that the stabilization of $T(\Gamma^\star)$ implies that of $\Gamma^\star$, it is necessary that there exist a class-$\mathcal{K}$ function $\alpha$ such that $\xi(x) \geq \alpha(\|x\|_{\Gamma^\star})$.

The computation, in step **S1**, of $\Gamma^\star$ can be performed using the zero dynamics algorithm described in [4], provided some mild regularity conditions hold. We now discuss the existence and derivation of the coordinate and feedback transformations that are required in step **S2** to get the normal form (2) with the property that $T(\Gamma^\star) = \{(\eta, \xi) : \xi = 0\}$. The transformations in question are guaranteed to exist locally around any point of $\Gamma^\star$ (see [9] and [7]) if and only if there exist functions $\alpha_1(x), \ldots, \alpha_l(x)$, $1 \leq l \leq m$, with the following properties. (a)

1) $\Gamma^\star \subset \{x : \alpha_1(x) = \cdots = \alpha_l(x) = 0\}$.
2) The "virtual" output $\alpha(x) = \mathrm{col}(\alpha_1(x), \ldots, \alpha_l(x))$ yields a uniform vector relative degree $\{k_1, \ldots, k_l\}$ on $\Gamma^\star$ and the indices $k_i$ are such that $k_1 + \cdots + k_l = n - n^\star$.

A good first guess for the required virtual output is the function $s(h(x))$, or a function defined using some of the components of $s(h(x))$, because it already satisfies property (a) above. If this guess doesn't work, then Theorem 3.2 in [9] (see also Theorem V.1 in [7]) gives necessary and sufficient checkable conditions for the existence of the required functions. More comments on the derivation of $\alpha_1, \ldots, \alpha_l(x)$ are found in [9]. Now suppose that $\alpha_1(x), \ldots, \alpha_l(x)$ have been found that satisfy properties (a) and (b). We show how they are used to derive the normal form (2). Let $D(x)$ be the decoupling matrix associated to the output $\alpha(x)$, i.e., the $l \times m$ matrix with components $D_{ij}(x) = L_{g_j} L_f^{k_i - 1} \alpha_i(x)$ which, by property (b), has rank $l$ on $\Gamma^\star$ and therefore also on a neighbourhood $\mathcal{N}$ of $\Gamma^\star$. Let $\beta(x) = [M(x)\ N(x)]$, where $M(x) := D^\top(x)(D(x)D^\top(x))^{-1}$ is the $m \times l$ right-inverse of $D(x)$, and $N(x)$ is a $m \times (m - l)$ smooth matrix-valued function whose columns span[3] the kernel of $D(x)$. Notice that $\beta(x)$ just defined is non-singular. Let $\alpha(x) = -\beta(x)\,\mathrm{col}(L_f^{k_1}\alpha_1, \ldots, L_f^{k_l}\alpha_l, 0_{m-l\times 1})$. Consider the feedback transformation $u = \alpha(x) + \beta(x)v$, where $v = \mathrm{col}(v^\pitchfork, v^\parallel)$, with $v^\pitchfork \in \mathbb{R}^l$ and $v^\parallel \in \mathbb{R}^{m-l}$. This feedback transformation and property (b) give

$$\begin{bmatrix} d^{k_1}\alpha_1/dt \\ \vdots \\ d^{k_l}\alpha_l/dt \end{bmatrix} = \begin{bmatrix} L_f^{k_1}\alpha_1 \\ \vdots \\ L_f^{k_l}\alpha_l \end{bmatrix} + D(x)(\alpha(x) + \beta(x)v) = v^\pitchfork.$$

Defining the map $x \mapsto \xi$ as

$$\xi := \mathrm{col}(\alpha_1, \ldots, L_f^{k_1-1}\alpha_1, \ldots, \alpha_l, \ldots, L_f^{k_l-1}\alpha_l)(x),$$

the above implies that $\dot\xi = A\xi + Bv^\pitchfork$, where $(A, B)$ is in Brunowský normal form with controllability indices $\{k_1, \ldots, k_l\}$. Next, following the ideas in the proof of Proposition 11.5.1 in [5], one finds that there exists a map $\eta = \varphi(x)$ mapping a neighbourhood of $\Gamma^\star$ onto $\Gamma^\star$ such that the transformation $T : x \mapsto (\eta, \xi)$ is a diffeomorphism

[3]Since $D(x)$ has constant rank around $\Gamma^\star$, for each point $p$ in $\Gamma^\star$ there exists a smooth matrix-valued function $N(x)$, defined in a neighbourhood of $p$, spanning the kernel of $D$. This isn't enough, as we want to define $N(x)$ over a neighbourhood of $\Gamma^\star$ on which $D$ has full rank (possibly the whole $\mathcal{N}$). If $\mathcal{N}$ is a contractible set (i.e., if it can be continuously deformed to a point), then in fact one can find $N(x)$ defined over the whole $\mathcal{N}$.

Fig. 1. The magnetic levitation system

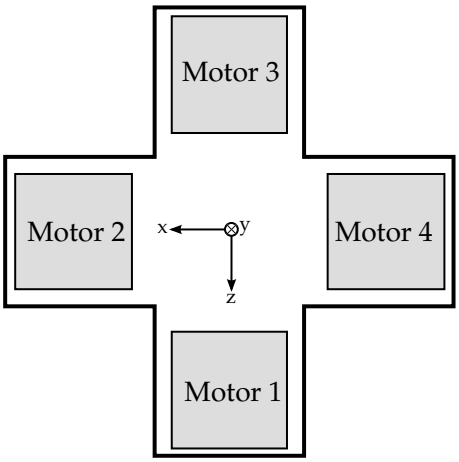


Fig. 2. Top view of the magnetic levitation system

mapping a neighbourhood of $\Gamma^\star$ onto a neighbourhood of $\Gamma^\star \times \mathbb{R}^{n-n^\star}$. In transformed coordinates, the dynamics have precisely the form (2). It can also be shown, using a straightforward argument found in the proof of Theorem 4.1 in [8], that $T(\Gamma^\star) = \{(\eta, \xi) : \xi = 0\}$. This concludes the derivation of the normal form in step **S2**.

## III. Experimental apparatus and model

### A. Hardware setup

The 5-DOF maglev positioning system, shown in Figure 1, was developed in collaboration with Quanser and is the evolution of two previous setups, a 2-DOF and a 3-DOF, described in [2]. The setup used in this research consists of four symmetrically placed iron-cored permanent magnet linear synchronous motors, or PMLSMs, shown from the top view in Figure 2. Each PMLSM is labeled Motor 1 to Motor 4, and consists of a stator and a mover. The stators are housed in a heavy stationary frame and each mover is positioned beneath its corresponding stator and affixed to an aluminium platen. Each stator exerts two orthogonal forces on the mover: a horizontal translational force and a vertical normal force. The aluminium platen is positioned below a stationary frame and rests on sets of linear guides[4] that allow the platen to move along two horizontal axes, one vertical axis, as well as rotate about the two horizontal axes (pitch and roll).

The system has a horizontal displacement range of $\pm 50$ mm along the X-axis and Z-axis, a vertical range of approximately 13 mm, and rotations about the X-axis and Z-axis of approximately $\pm 3$ mrad and $\pm 14$ mrad, respectively. Let $\mathcal{T} = [0.018, 0.031] \times [-0.05, 0.05] \times [-0.05, 0.05]$ and $\mathcal{R} = [-0.003, 0.003] \times [-0.014, 0.014]$ denote the allowable operating range of the translational and rotational subsystems measured in meters and radians, respectively.

### B. Mathematical model

The mathematical model of the forces produced by a PMLSM was reported in [6]. Using this model it is a simple matter to derive the dynamics describing the translations and two rotations of the platen. The detailed derivation is found in [3]. For the sake of clarity and conciseness, we will not present the cumbersome expressions of the forces and the derivation of the mathematical model. We will rather focus on presenting its basic structure.

We denote by $x_1$, $x_3$, and $x_5$ the $Y$, $X$, and $Z$-axes displacements of the centre of mass of the platen, respectively, and by $x_2$, $x_4$, and $x_6$ their velocities. Note that $(x_1, x_3, x_5) \in \mathcal{T}$. Let $x_7$ and $x_9$ denote the rotation angles of the platen about the $X$ and $Z$-axes, respectively, and by $x_8$ and $x_{10}$ the corresponding angular velocities. We have that $(x_7, x_9) \in \mathcal{R}$. Our convention is that when $x_1 = 0.025$ and $x_3 = x_5 = x_7 = x_9 = 0$ the platen is placed in the centre of its displacement range and it is leveled with the ground.

The physical inputs to the system are the applied three-phase currents to each of the PMLSMs. It is customary to represent three-phase currents of motor $k$, $k = 1, \ldots, 4$, using their direct and quadrature components, which we denote by $i_{d_k}$ and $i_{q_k}$. Having eight control inputs, the system is overactuated. We now briefly describe how to eliminate the overactuation. Set $u_x := i_{q_2} = i_{q_4}$, $u_z := i_{q_1} = i_{q_3}$, to make sure that when the platen is leveled with the ground the horizontal forces produced by motor pairs (2,4) and (1,3) are the same. We further set $u_y := i_{d_1} + i_{d_3} = i_{d_2} + i_{d_4}$, $u_\phi := i_{d_1} - i_{d_3}$, $u_\theta := i_{d_2} - i_{d_4}$. The definition of $u_y$ guarantees that when the platen is leveled with the ground motor pairs (1,3) and (2,4) produce the same lift force. We thus have five control inputs $(u_x, u_z, u_y, u_\phi, u_\theta)$ that actuate 5-DOFs.

With this definition, a simplified[5] mathematical model of the system has the form (3). The state space of the system is $\mathcal{X} := \mathbb{R}^6 \times \mathbb{S}^1 \times \mathbb{R} \times \mathbb{S}^1 \times \mathbb{R}$, where $\mathbb{S}^1$ denotes the unit circle. The system output is given by the three displacements, $h(x) := \mathrm{col}(x_1, x_3, x_5)$. For the remainder of this paper we will call the $(x_1, x_2, x_3, x_4, x_5, x_6)$ subsystem the *translational subsystem* and $(x_7, x_8, x_9, x_{10})$ the *rotational subsystem*.

[4]The linear guides do not provide any actuation force to the platen other than friction (a disturbance) and are currently required to maintain proper alignment of the platen and, most importantly, facilitate the placement of sensors used to measure displacements and rotations of the platen.

[5]In reality, the mathematical model of the plant is not affine in the control inputs $u_y, u_\phi$, and $u_\theta$, due to the presence of quadratic expressions involving these currents. However, the analysis in [3] shows that the control-affine approximation of the model describes the dynamics of the control system sufficiently well for control purposes.

$$
\begin{aligned}
\dot{x}_1 &= x_2 \\
\dot{x}_2 &= a_1(x_1, x_7, x_9, u_x, u_z) + a_2(x_1, x_7, x_9)u_y \\
&\quad + a_3(x_1, x_7)u_\phi + a_4(x_1, x_9)u_\theta \\
\dot{x}_3 &= x_4 \\
\dot{x}_4 &= p(x_1, x_9)u_x \\
\dot{x}_5 &= x_6 \\
\dot{x}_6 &= q(x_1, x_7)u_z \\
\dot{x}_7 &= x_8 \\
\dot{x}_8 &= b_1(x_1, x_7, u_z) + b_2(x_1, x_7)u_y + b_3(x_1, x_7)u_\phi \\
\dot{x}_9 &= x_{10} \\
\dot{x}_{10} &= c_1(x_1, x_9, u_x) + c_2(x_1, x_9)u_y + c_3(x_1, x_9)u_\theta.
\end{aligned} \tag{3}
$$

All functions in the above model are smooth. Their salient properties are listed below

- $b_1(x_1, 0, u_z) \equiv b_2(x_1, 0) \equiv c_1(x_1, 0, u_x) \equiv c_3(x_1, 0) \equiv 0$.
- The functions $p(x_1, x_9), q(x_1, x_7), b_3(x_1, x_7), c_3(x_1, x_9)$ do not vanish on $\mathcal{T} \times \mathcal{R}$.
- Letting

$$
K(x) := \begin{bmatrix} a_2(x_1, x_7, x_9) & a_3(x_1, x_7) & a_4(x_1, x_9) \\ b_2(x_1, x_7) & b_3(x_1, x_7) & 0 \\ c_2(x_1, x_9) & 0 & c_3(x_1, x_9) \end{bmatrix},
$$

the matrix $K(x)$ is nonsingular on $\mathcal{T} \times \mathcal{R}$.

## IV. Path following control design

We want to solve the path following control problem, formulated in Section II, with path $\gamma$ given by a closed Jordan curve in the output space. To concretely illustrate our design, we pick an ellipse not leveled with the ground,

$$
\gamma := \left\{ (y_1, y_2, y_3) \in \mathbb{R}^3 : s_1(y) = s_2(y) = 0 \right\}, \tag{4}
$$

$s_1(y) := y_2^2 + y_3^2 - 0.03^2$, $s_2(y) := -18y_1 + 3y_2 + 0.45$, but our procedure can be applied to any other embedded path that is expressible as the zero level set of a function. The ellipse, shown in Figure 3, covers most of the operating range $\mathcal{T}$ for the displacements. The controller must meet objectives

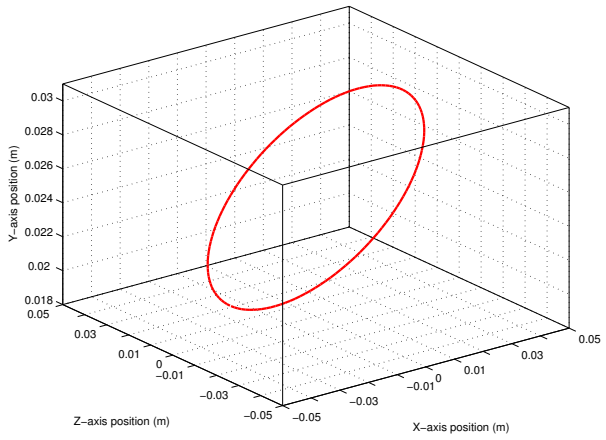


Fig. 3. The desired path $\gamma$. The box represents the operating range $\mathcal{T}$

**P1-P3** in Section II with **P3** specialized to this application as follows,

**P3** On the path $\gamma$, $(x_1(t), x_3(t), x_5(t))$ tracks a desired speed profile. Moreover, the rotational dynamics are regulated to zero, i.e., $(x_7(t), x_8(t), x_9(t), x_{10}(t)) \to 0$ as $t \to \infty$.

### A. Preliminary feedback transformation

The first step in controller design is to observe that the plant (3) is feedback linearizable. The feedback transformation

$$
\begin{aligned}
\begin{bmatrix} u_x \\ u_z \end{bmatrix} &= \begin{bmatrix} u_2/p(x_1, x_9) \\ u_3/q(x_1, x_7) \end{bmatrix} \\
\begin{bmatrix} u_y \\ u_\phi \\ u_\theta \end{bmatrix} &= K(x)^{-1} \begin{bmatrix} u_1 - a_1(x_1, x_7, x_9, u_x, u_z) \\ u_4 - b_1(x_1, x_7, x_9, u_z) \\ u_5 - c_1(x_1, x_9, u_x) \end{bmatrix},
\end{aligned} \tag{5}
$$

gives five decoupled double-integrators with input $u := (u_1, \ldots, u_5)$,

$$
\dot{x} = \hat{A}x + \hat{B}u \tag{6}
$$

where $\hat{A}$ and $\hat{B}$ are in Brunowský canonical form. We next apply the procedure presented in Section II to system (6) with path (4).

### B. S1: Finding the path following manifold

The path following manifold $\Gamma^\star$ is the maximal control invariant subset of $\Gamma = \{x : s_1(h(x)) = 0, s_2(h(x)) = 0\}$, with $s_1(h(x)) = x_3^2 + x_5^2 - 0.03^2$ and $s_2(h(x)) = -18x_1 + 3x_3 + 0.45$. In this case, the task of finding $\Gamma^\star$ is straightforward because the virtual output $\hat{y} := \mathrm{col}(s_1(h(x)), s_2(h(x)))$ yields a well-defined vector relative degree of $\{2, 2\}$ on $\mathcal{X}/\{x : x_3 = x_5 = 0\}$, since the decoupling matrix

$$
D(x) = \begin{bmatrix} 0 & 2x_3 & 2x_5 & 0 & 0 \\ -18 & 3 & 0 & 0 & 0 \end{bmatrix}
$$

has full rank on $\mathcal{X}/\{x : x_3 = x_5 = 0\}$. Therefore the path following manifold has dimension $n^\star = 6$ and is given by

$$
\begin{aligned}
\Gamma^\star = \Big\{ x \in \mathcal{X} : & x_3^2 + x_5^2 - 0.03^2 = -18x_1 + 3x_3 + 0.45 = \\
& 2x_3x_4 + 2x_5x_6 = -18x_2 + 3x_4 = 0 \Big\}.
\end{aligned} \tag{7}
$$

### C. S2: Transverse feedback linearization

Since the virtual output $\hat{y} = \mathrm{col}(s_1(h(x)), s_2(h(x)))$ yields a well-defined vector relative degree, the derivation of the normal form (2) amounts to standard input-output feedback linearization. Following the procedure for deriving the normal form outlined in Section II, let $\beta(x) = [M(x) \quad N(x)]$, where $M(x) = D^\top(x)(D(x)D^\top(x))^{-1}$ is the right-inverse of $D(x)$ and the columns of

$$
N(x) = \left[\begin{array}{c|c} x_5 & \\ 6x_5 & 0_{3\times 2} \\ -6x_3 & \\ \hline 0_{2\times 1} & I_2 \end{array}\right]
$$

span the kernel of $D(x)$, and define the feedback transformation

$$\begin{aligned} u &= -\beta(x)\,\mathrm{col}(2(x_4^2+x_6^2),0,0,0,0)+\beta(x)v,\\ v &= (v_1^{\pitchfork},v_2^{\pitchfork},\hat{v}_1^{\parallel},v_2^{\parallel},v_3^{\parallel}). \end{aligned} \tag{8}$$

Notice that this feedback transformation is regular on $\mathcal{X}/\{x : x_3 = x_5 = 0\}$. Next, the state of the transversal subsystem is defined as

$$\xi := \begin{bmatrix} x_3^2+x_5^2-0.03^2\\ 2x_3x_4+2x_5x_6\\ -18x_1+3x_3+0.45\\ -18x_2+3x_4 \end{bmatrix}. \tag{9}$$

We complete the coordinate transformation by means of the map $x \mapsto \eta$ defined below,

$$\begin{aligned} \eta_1 &= \arg(x_3+ix_5)\\ \eta_2 &= (x_3x_6-x_4x_5)/(x_3^2+x_5^2)\\ \eta_3 &= x_7\\ \eta_4 &= x_8\\ \eta_5 &= x_9\\ \eta_6 &= x_{10}. \end{aligned} \tag{10}$$

The state $\eta_1$ is the angle formed by the projection of the centre of mass of the platen onto the $X-Z$ plane and the $X$-axis, and $\eta_2$ represents the corresponding angular velocity. Therefore, when $\xi = 0$, i.e., when the centre of mass of the platen is on $\gamma$, the pair $(\eta_1,\eta_2)$ completely describes the position and velocity of the platen. On the other hand, $\eta_3,\eta_4,\eta_5,\eta_6$ are simply the states of the rotational subsystem. The transformation $T : x \mapsto (\eta,\xi)$ defined by (9) and (10) is a diffeomorphism of $\mathcal{X}/\{x : x_3 = x_5 = 0\}$ onto its image and it yields the desired normal form,

$$\begin{aligned} \dot{\eta}_1 &= z_2\\ \dot{\eta}_2 &= \phi(x,v_1^{\pitchfork},v_2^{\pitchfork})-6\hat{v}_1^{\parallel}\\ \dot{\eta}_3 &= z_4\\ \dot{\eta}_4 &= v_2^{\parallel}\\ \dot{\eta}_5 &= z_6\\ \dot{\eta}_6 &= v_3^{\parallel}\\ \dot{\xi} &= A\xi+Bv^{\pitchfork}. \end{aligned}$$

where $\phi(x,v_1^{\pitchfork},v_2^{\pitchfork})$ is a smooth function defined on $\mathcal{X}/\{x : x_3 = x_5 = 0\}$. Interestingly, the system above is feedback equivalent to a linear time-invariant system. For, by letting

$$\hat{v}_1^{\parallel} = 1/6(\phi(x,v_1^{\pitchfork},v_2^{\pitchfork})-v_1^{\parallel}), \tag{11}$$

we obtain the linear time-invariant system

$$\begin{aligned} \dot{\eta} &= A^{\star}\eta+B^{\star}v^{\parallel}\\ \dot{\xi} &= A\xi+Bv^{\pitchfork}, \end{aligned} \tag{12}$$

where $(A^{\star},B^{\star})$ and $(A,B)$ are in Brunowský normal form and represent, respectively, three decoupled double-integrators and two decoupled double-integrators.

### D. S3: Transversal control design

We stabilize the origin of the transversal subsystem in (12), therefore meeting design goals **P1** and **P2**, by means of two parallel PID compensators,

$$\begin{aligned} v_1^{\pitchfork}(\xi) &= -K_{11}\xi_1-K_{12}\xi_2-K_{13}\int_0^t \xi_1(\tau)d\tau\\ v_2^{\pitchfork}(\xi) &= -K_{21}\xi_3-K_{22}\xi_4-K_{23}\int_0^t \xi_3(\tau)d\tau. \end{aligned}$$

Since $v_1^{\pitchfork}(0) = v_2^{\pitchfork}(0) = 0$, $\xi = 0$ is an equilibrium of the closed-loop transversal subsystem in (12), and thus $\Gamma^{\star}$ is an invariant set for the closed-loop system. In other words, the controller above meets goal **P2**. The positive gains $K_{ij}$ are selected using LQR design with manual tuning of the weight matrices.

### E. S4: Tangential control design

We now design a tangential controller for the $\eta$-subsystem in (12) that meets objective **P3**. Recalling the definition of $\eta$ in (10), making sure that, on $\gamma$, the centre of mass of the platen $(x_1,x_2,x_3)$ tracks a desired speed profile is equivalent to making sure that the angular velocity $\eta_2$ approaches a desired reference profile $\eta_2^{\mathrm{ref}}(t)$, which can be achieved by means of a simple proportional feedback with feedforward action. Furthermore, regulating the rotational dynamics corresponds to stabilizing the origin of the subsystem with states $(\eta_3,\eta_4,\eta_5,\eta_6)$, which can be achieved by means of two PID compensators. In the light of the above, the tangential controller

$$\begin{aligned} v_1^{\parallel}(\eta) &= \dot{\eta}_2^{\mathrm{ref}}(t)+K_3(\eta_2-\eta_2^{\mathrm{ref}}(t))\\ v_2^{\parallel}(\eta) &= -K_{41}\eta_3-K_{42}\eta_4-K_{43}\int_0^t \eta_3(\tau)d\tau\\ v_3^{\parallel}(\eta) &= -K_{51}\eta_5-K_{52}\eta_6-K_{53}\int_0^t \eta_5(\tau)d\tau \end{aligned}$$

meets design goal **P3**. The positive gains in the above controller are chosen using LQR design with manual tuning of the weight matrices in order to stabilize the rotational dynamics.

## V. Experimental Results

We define the instantaneous "path error", denoted $e(t)$, as the minimum Euclidean distance of the center of mass of the platen to the path at time $t$, $e(t) := \|(x_1(t),x_3(t),x_5(t))\|_{\gamma}$. The average path error over a finite time interval $[0,T]$ is

$$\bar{e}(T) := \frac{1}{T}\int_0^T e(\tau)d\tau.$$

The average path error is the benchmark throughout the tuning process.

### A. Experiment 1

After tuning the proportional controller for the tangential control, we ran a test consisting of a series of constant angular velocity commands $\{\pi/2,\pi/4,\pi/8,-\pi/8,-\pi/4,-\pi/2\}$

rad/s in order to tune the LQR gain matrices for the transversal control. For each velocity, the platen was moved through two circuits around the path before switching to the next velocity command. The initial average path error for this test was over $300\mu$m, and after tuning the average path error was reduced to approximately $41\mu$m. Figure 4 shows the position response of the system after tuning in XYZ Figure 5 shows the measured path error during the test. The performance is clearly satisfactory.

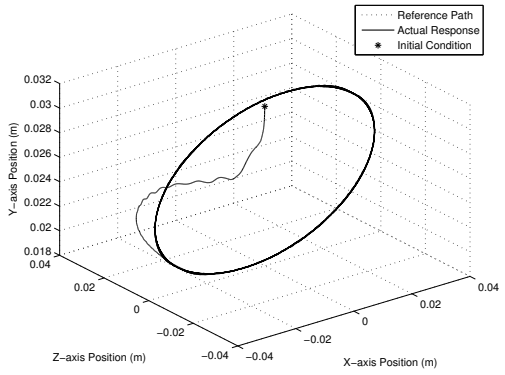


Fig. 4. Position response of the path following controller.

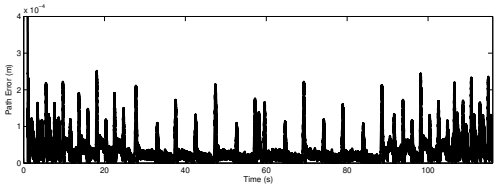


Fig. 5. Path error measured for the path following controller at various velocities

### B. Experiment 2

We further tested the accuracy of the path following controller by running longer trials at constant velocities ranging from $\pi/8$ rad/s to $2\pi$ rad/s and recording the average path error with $T = 60$ seconds for each velocity. Figure 6 summarize the results from this test. We observe a large increase in average path error as the speed increases.

### C. Discussion

We observed that there was a significant friction effect at certain points where the platen's motion along an axis stops and changes direction. We call these *turn-around points*. We say that this is predominantly a friction effect for two reasons: 1) the effect is symmetrical and depends on the direction of travel, and 2) the effect is less predominant at larger velocities when the platen has more persistency of motion. Figure 7 illustrates the effect (before controller tuning) at velocities $\pi/8$ and $-\pi/8$.

Another undesirable effect that we observe is a slight coupling between the $\eta$ and $\xi$ dynamics, that theoretically

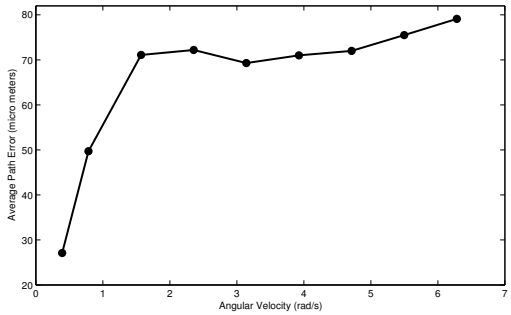


Fig. 6. Average path error measured over 60 seconds for various angular velocities

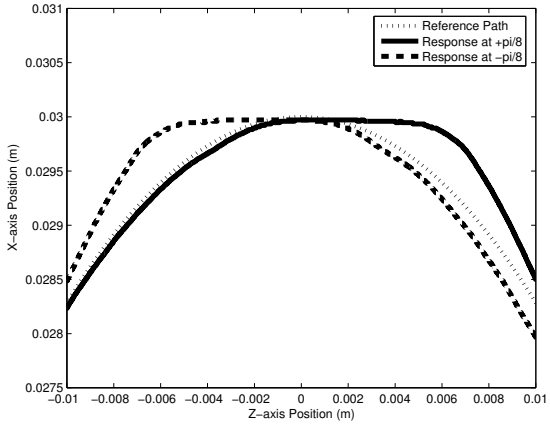


Fig. 7. Effect of friction at a turn-around point for small velocities before tuning

(see (12)) are decoupled. This coupling manifests itself by an increase in the average path error at large angular velocities $\eta_2$. This is evidenced in Figure 6 which show the measured average path errors for various angular velocities.

## REFERENCES


[1] A. Banaszuk and J. Hauser. Feedback linearization of transverse dynamics for periodic orbits. *Systems and Control Letters*, 26(2):95–105, Sept. 1995.

[2] O. Brydon, M. Maggiore, and J. Apkarian. A high-precision, magnetically levitated positioning stage. *IEEE Control Systems Magazine*, 26(03):82–95, June 2006.

[3] C. Fulford. Control of a high-precision positioning system using magnetic levitaion. Master's thesis, University of Toronto, 2007.

[4] A. Isidori. *Nonlinear Control Systems*. Springer, New York, $3^{rd}$ edition, 1995.

[5] A. Isidori. *Nonlinear Control Systems II*. Springer-Verlag, London, 1999.

[6] M. Maggiore and R. Becerril. Modeling and control design for a magnetic levitation system. *Int. J. Control*, 77(10):964–977, 2004.

[7] C. Nielsen and M. Maggiore. Further results on transverse feedback linearization of multi-input systems. In *Proc. of the IEEE Conference on Decision and Control*, pages 3819–3824, San Diego, CA, USA, December 2006.

[8] C. Nielsen and M. Maggiore. Output stabilization and maneuver regulation: A geometric approach. *Systems Control Letters*, 55:418–427, 2006.

[9] C. Nielsen and M. Maggiore. On local transverse feedback linearization. *SIAM J. Control and Optimization*, 47(5):2227–2250, 2008.